ACS Chemical Neuroscience

Research Article

pubs.acs.org/chemneuro

Protonation State of a Conserved Acidic Amino Acid Involved in Na^+ Binding to the Glutamate Transporter EAAC1

Juddy Mwaura, Zhen Tao,[†] Herbert James, Thomas Albers, Alexander Schwartz, and Christof Grewer*

Department of Chemistry, Binghamton University, Binghamton, New York 13902, United States

Supporting Information

ABSTRACT: Substrate transport by glutamate transporters is coupled to the co-transport of 3 Na^+ ions and counter-transport of 1 K^+ ion. The highly conserved Asp454, which may be negatively charged, is of interest as its side chain may coordinate cations and/or contribute to charge compensation. Mutation to the nonionizable Asn resulted in a transporter that no longer catalyzed forward transport. However, Na^+/glutamate exchange was still functional, as demonstrated by the presence of transient currents following rapid substrate application and voltage jumps. While the kinetics of Na^+/glutamate exchange were slowed, the apparent valence (z) of the charge moved in EAAC1 D454N (0.71) was similar to that of EAAC1 WT (0.64). Valences calculated using the Poisson−Boltzmann equation were close to the experimental values for EAAC1 D454N (0.55), and with D454 protonated (0.45). In addition, pK_a calculations performed for the bacterial homologue GltPh revealed a highly perturbed pK_a (7.6 to >14) for D405 residue (analogous to D454), consistent with this site being protonated at physiological pH. In contrast to the D454N mutation, substitution to alanine resulted in a transporter that still bound glutamate, but could not translocate it. The results are consistent with molecular dynamics simulations, showing that the alanine but not the asparagine mutation resulted in defective Na^+ coordination. Our results raise the possibility that the protonated state of D454 supports transporter function.

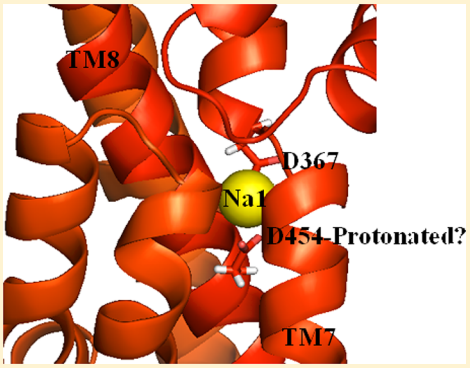

KEYWORDS: *Glutamate transporter, mutagenesis, Na^+ coupling, secondary-active transport, electrophysiology*

The neuronal glutamate transporter EAAC1 (Excitatory Amino Acid Carrier 1) mediates the active transmembrane transport of glutamate, by coupling it to the co-transport of three Na^+ ions down their concentration gradient.[1−3] It also co-transports one proton, and one K^+-ion is counter-transported in a step that is separate from the Na^+/glutamate translocation step.[3,2,4,5] A bacterial homologue of the mammalian glutamate transporters, GltPh from *Pyrococcus horikoshii*, has been crystallized, providing a high resolution structure.[6] In analogy with the mammalian transporters, GltPh is thought to co-transport three Na^+ ions with one acidic amino acid molecule.[7−9] However, only two Na^+ binding sites, termed Na1 and Na2 sites, are resolved in the crystal structure.[7] The location of the potential third Na^+ binding site (Na3 site), which is most likely required to support the 3:1 Na^+-glutamate stoichiometry, is not known, but mutagenesis and molecular dynamics studies point to two possible locations, one deeply buried in the membrane and the other one closer to the substrate binding site.[8,10−12]

Several studies give hints to the nature of the Na1 binding site. Both the crystal structure and molecular dynamics indicate that a highly conserved aspartate residue, D454 in EAAC1, coordinated Na^+ through its side chain.[7,10] D454 has been mutated to several charged and noncharged amino acid residues.[13] In particular, it was found that a transporter with the conservative D454N mutation could still exchange substrate across the membrane, based on equilibrium exchange flux experiments.[13] Furthermore, the D454N mutation did not interfere with the ability of Na^+ to activate the Na^+-dependent anion conductance[13] and the apparent sodium affinity was unaffected. However, the interaction with K^+ seemed to be impaired, since the D454N mutant transporter was unable to sustain net forward transport of substrate and application of extracellular K^+ was unable to mediate reverse transport.[13] The apparent lack of a substantial effect of the D454N mutation on the Na^+/glutamate dependent steps of the transport cycle is surprising, considering that this mutation might affect the charge of the cation binding site(s) or could lead to a disruption of the electrostatic contribution to the conformational changes associated with glutamate translocation.

To answer open questions concerning the contribution of electrostatics, we performed in this work a more detailed characterization of mutations to the D454 position. Rapid kinetic analysis based on glutamate concentration jumps, as well as on voltage jumps, indicates that the charge movement associated with glutamate translocation is altered only to a minor extent by the D454N mutation, but that charge movement is abolished by the D454A mutation. In contrast,

Received: September 18, 2012
Accepted: October 19, 2012
Published: October 19, 2012

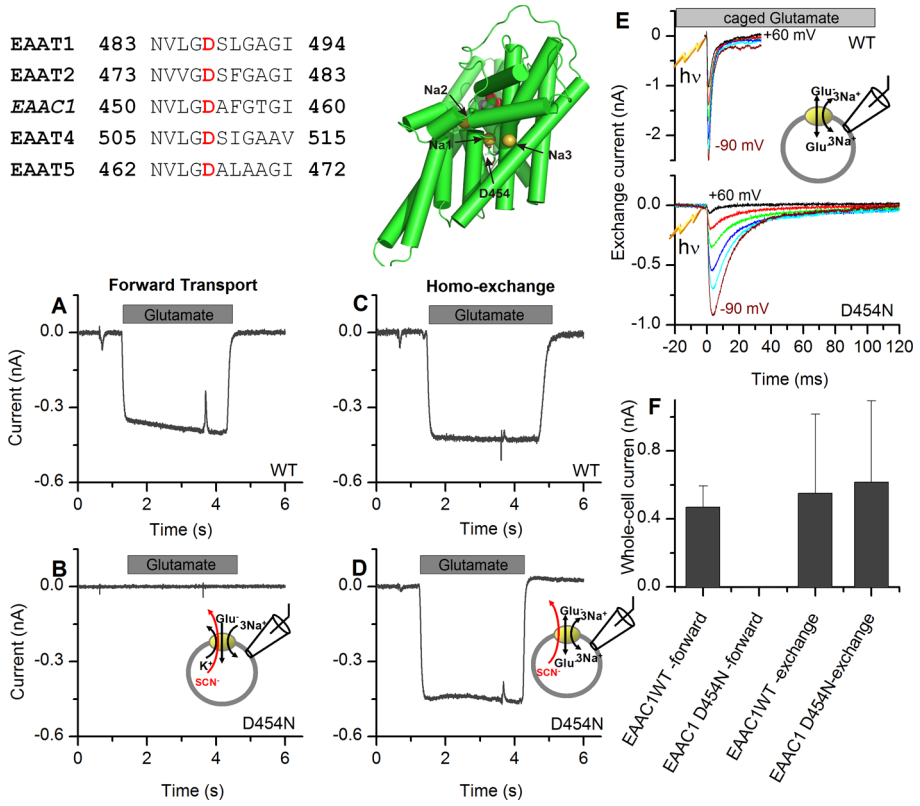

Figure 1. Forward transport is impaired, but homoexchange is still functional in EAAC1 D454N. (Insets) Sequence alignment and structure showing the highly conserved Asp 454 within the EAAT family of transporters, as well as the three proposed Na^+ binding sites, Na1−Na3. (A) Typical glutamate induced anion currents obtained in the forward transport mode (120 mM KSCN intracellular) for EAAC1 WT. (B) Transport currents were abolished in EAAC1 D454N under similar recording conditions as in (A). (C and D) Typical anion currents obtained in exchange mode (120 mM NaSCN and 10 mM glutamate intracellular) for (C) EAAC1 WT and (D) EAAC1 D454N. (F) Average anion currents obtained in forward transport and exchange mode. (E) Typical transient currents obtained with EAAC1 WT (top) and D454N (bottom) following rapid glutamate application by laser photolysis of 1 mM MNI caged glutamate at $t = 0$, at different voltages (−90 to +60 mV). The intracellular solution contained 140 mM NaMes and 10 mM glutamate. The transient currents demonstrate that Na^+/glutamate exchange is still functional in EAAC1 D454N.

a transporter with the D454K mutation still showed substrate-induced charge movement. The pH dependence of exchange was not altered by the D454N mutation, but a moderate reduction in the apparent affinity of K^+ binding was observed. The results are consistent with calculations of the pK_a of the D454 residue, as well as molecular dynamics simulations, which point to at least partial activity of EAAC1 with D454 existing in the protonated form.

RESULTS

Relocation of the Empty Transporter Is Impaired in EAAC1 D454N. To test the effect of introducing a charge-neutralizing mutation at position 454 on the EAAC1 transport cycle, we carried out current recordings in the forward transport mode (high intracellular K^+) and homoexchange mode (no intracellular K^+, highly anion conducting state). Anion currents catalyzed by glutamate application to the wild-type transporter under forward transport conditions were found to be absent in EAAC1 D454N (Figure 1A and B). However, anion currents similar to those of the wild-type transporter were obtained under homoexchange conditions (Figure 1C and D). Transient transport currents associated with Na^+/glutamate exchange were also obtained following rapid application of glutamate by laser pulse photolysis of 1 mM caged glutamate in the homoexchange mode (Figure 1E), decaying with two exponential components. These transient currents were similar in their magnitude to those observed in EAAC1 WT[14] but decayed with 6-fold slower time constants for the fast phase, and 3-fold slower time constant for the slow phase compared to EAAC1 WT. Together, these results indicate that the Na^+/glutamate translocation steps are still functional, but slowed in EAAC1 D454N, whereas the K^+ induced relocation of the empty transporter is impaired, as has been previously proposed for this mutant transporter based on current recording and flux measurements.[13,15] Therefore, all subsequent experiments were carried out under Na^+/glutamate exchange conditions.

Voltage Dependence of the Charge Movement Associated with Glutamate Translocation Is Unchanged by the D454N Mutation. In order to establish if the charge-neutralizing mutation at position 454 affects the voltage dependence of the charge moved during Na^+/glutamate translocation, voltage jumps (−90 to +60 mV) were applied to perturb the Na^+/glutamate exchange equilibrium (Figure 2A), followed by analysis of the charge moved after the perturbation. As expected from the concentration jump analysis (Figure 1E), DL-*threo*-β-benzyloxyaspartic acid (TBOA)-sensitive transient currents associated with electrogenic relaxation to a new exchange equilibrium were observed in both the wild-type and EAAC1 D454N (Figure 2A and D), which were not caused by changes in the electrical parameters of the cell during the voltage jump procedure, as shown in Figure 2B and E. A fit to a Boltzmann-like function (eq 2) revealed that the charge (Q) moved in EAAC1 D454N under these conditions showed a

dx.doi.org/10.1021/cn300163p | ACS Chem. Neurosci. 2012, 3, 1073−1083

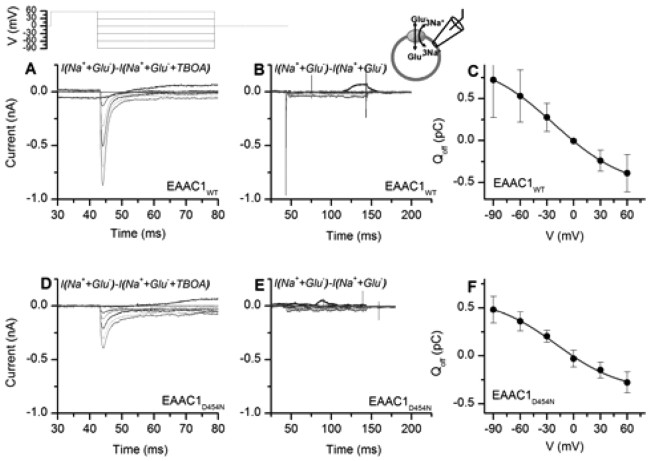

Figure 2. D454 to N exchange has no effect on voltage dependence of exchange. (A) EAAC1-specific transient currents obtained in response to the voltage jump protocol (top panel) (−90 to 60 mV) in homoexchange mode. The pipet solution contained 120 mM NaMes and 10 mM glutamate; the extracellular solution contained 140 mM Na^+ and 1 mM glutamate. TBOA blocks the EAAC1-specific component of the current, and $I(Na^+ + Glu^-) - I(Na^+ + Glu^- + TBOA)$ represents the current in the presence of 140 mM Na^+ + 1 mM glutamate from which the current in the presence of 140 mM Na^+ + 1 mM glutamate + 200 μM TBOA was subtracted. (B) To test for changes in membrane capacitance during the voltage jump protocol, currents before and after TBOA application were subtracted from each other ($I(Na^+ + Glu^-) - I(Na^+ + Glu^-)$). The currents showed no difference. (D and E) Results obtained for EAAC1 D454N under similar conditions as in (A). (C and F) Charge movement (Q_{off}) was obtained by integrating the off response measured from EAAC1 D454N and EAAC1 WT. The solid lines represent fits to the Boltzmann equation, with an apparent valence of 0.6 and midpoint potential of −21.6 mV for EAAC1 WT, and an apparent valence of 0.7 and midpoint potential of −18.9 mV for EAAC1 D454N.

dependence on the transmembrane potential similar to that of EAAC1 WT (Figure 2C and F). An apparent valence of 0.64 was obtained for EAAC1 WT and 0.71 for EAAC1 D454N. The midpoint potential (V_Q) was also found to be within the same range as that of the wild-type transporter, with $V_Q = -22 \pm 1$ mV for EAAC1 WT and -19 ± 7 mV for EAAC1 D454N. These results suggest that charge neutralization in position 454 does not strongly affect the electrostatics of the translocation reaction, either because the Asn side-chain mimics an Asp^-/Na^+ pair or because Asp is protonated and, therefore, neutral. The differentiation between these possibilities will be described in the Discussion.

Calculations of pK_a Values Indicate that D454 May Be Protonated. To gain insight into the protonation state, we calculated the pK_a values of conserved, ionizable side chains in the transmembrane domain, using an empirical (PROPKA)[16] as well as a Poisson−Boltzmann-based method.[17] pK_a calculations were performed for GltPh, in which the E373 residue of mammalian transporters is not conserved (GltPh has a glutamine in position 318). Thus, Q318 was not included in the analysis. While the protonation state of most side chains remained unchanged from what it would be in water, the pK_a values of the D312 and particularly the D405 side chains (corresponding to D367 and D454 in EAAC1) were shifted to higher values (Table 1). While pK_a values for D312 mostly predict deprotonated, negatively charged state of the side chain at pH 7.4, the calculated pK_a of D405 was in the range of 7.6 to

Table 1. Theoretical Predictions of pK_a Values of Conserved Ionizable Side Chains of the GltPh 2NWX Structure, as Well as the 2NWX apo Form, MD-Simulated for 8 ns in a Full Membrane-Explicit Water Environment after Removal of Na^+ Ions and the Substrate[a]

	2NWX apo (after 8 ns MD simulation)			2NWX Na_2-bound		
	MCCE			MCCE		
amino acid	$\varepsilon_P = 4$	$\varepsilon_P = 8$	PROPKA	$\varepsilon_P = 4$	$\varepsilon_P = 8$	PROPKA
D312	<0	2.3	4.7	8.9	7.4	5.8
D390	0.3	1.3	3.1	4.5	1.7	4.2
D394	2.9	2.8	4.3	0.13	2.4	5.5
R397	>14	>14	14.8	>14	>14	15.6
D405	9.7	7.6	7.6	>14	13.2	8.3

[a] pK_a values were calculated based on the PB equation (MCCE) or an empirical PROPKA (version 3.1) method. ε_P is the dielectric coefficient of the protein.

>14, suggesting that this side chain should be protonated under physiological conditions. In particular, D405 is predicted to be still protonated in the *apo*-state of the transporter, in which the Na1 site is accessible to water (Table 1). These results are in agreement with previous mutagenesis studies showing an absence of effect of the charge-neutralizing mutation of D454 to asparagine on Na^+ binding, as well as substrate exchange.[15,13]

Affinity for Glutamate and pH Dependence Are Unchanged by D454N Mutation. Although the transporter was defective in K^+-induced relocation, the apparent affinity for glutamate was not significantly affected by introduction of the nonionizable Asn side-chain. Na^+-dependent anion currents following glutamate concentration jumps yielded a dose dependent relationship, with a K_m of 19.8 ± 3.8 μM (wild-type transporter = 14 ± 1 μM) (Figure 3A).

Glutamate transport is accompanied by cotransport of a proton, resulting in intracellular acidification.[2,18] Protonation of wild-type EAAC1, presumably at E373, results in increased apparent affinity for glutamate.[18] Consistently, the apparent affinity of EAAC1 D454N for glutamate was found to be pH dependent (Figure 3B), with K_m increasing from 30 ± 3 μM at pH 6.0 to 144 ± 55 μM at pH 9.0. This pH dependence of K_m is very similar to that of EAAC1 WT, indicating that Asp 454 is not involved in proton binding/transport, as quantified using a semilogarithmic plot of the K_m vs pH (Figure 3B). Analysis of this plot yielded the dissociation constant for the substrate, K_s = 16.6 ± 6.7 μM, and the proton, $K_H = 2.3 \times 10^{-8} \pm 9.7 \times 10^{-9}$ M. This is consistent with an ionizable residue with a pK_a of 7.6 within the protein. Watzke et al. reported pK_a = 8 for the ionizable residue and K_s = 5.5 μM in EAAC1 WT.[18] Therefore, neutralization of Asp 454 through site-directed mutagenesis does not significantly affect the pH dependence of the transporter, indicating that D454 does not change protonation state within the pH 6−9 range, or that a change of protonation state has no functional consequence.

Prediction of Valences Using Poisson−Boltzmann Analysis. So far, results from experiments and calculations indicate that D454 may be protonated at physiological pH. To test this hypothesis, we analyzed valences computed for the major outward- to inward-facing transition for wild-type and mutant transporters (Table 2), using numerical solution of the Poisson−Boltzmann equation. In the presence of an occupied Na1 site, protonation of D454 resulted in an increase of the valence from 0.16 to 0.45, as expected for the elimination of a

dx.doi.org/10.1021/cn300163p | ACS Chem. Neurosci. 2012, 3, 1073−1083

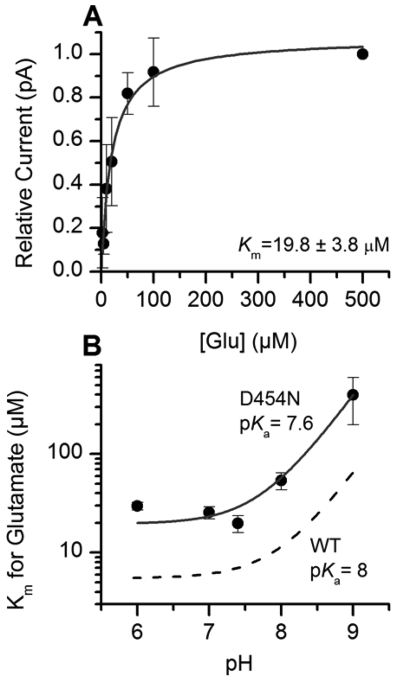

Figure 3. Glutamate affinity and pH dependence of the transporter are not affected by mutation of D454 to N. (A) The apparent affinity for glutamate (K_m) was determined in homoexchange mode. The intracellular solution contained 120 mM NaSCN and 10 mM glutamate, and the extracellular solution contained 140 mM NaMes (V = 0 mV). (B) Semilogarithmic plot of K_m as a function of extracellular pH. The solid line represents a fit to $K_S(K_H + [H]/[H])$ with K_s = 16.6 ± 6.7 μM and $K_H = 2.3 \times 10^{-8} \pm 9.7 \times 10^{-9}$ M. The dashed line represents a fit to EAAC1 WT data from ref 18.

Table 2. Predicted Valences for the Outward-to-Inward-Facing Transition for Wild-type and Several Mutant EAAC1s in the Absence or Presence of Bound Na^+ in the Na1 Site[a]

	wild-type	D454-prot	D454N	D454A	D454K
fully loaded	0.16	0.45	0.55	0.54	0.95
no Na1 bound	−0.4	0.08	0.09	0.09	0.49

[a]In D454-prot, the aspartate side chain was protonated. The substrate binding site and the Na2 and Na3 sites were occupied. The valences were calculated using APBSmem.

movable negative charge within the transmembrane domain (Table 2). The valence for the conformational change in the D454N mutant transporter (0.55) was similar to that of the protonated wild-type transporter and was reduced to 0.09 upon removal of the Na^+ ion in the Na1 site. However, this valence was too low compared to the experimentally determined value (0.71), suggesting that presence of net positive charge in the Na1 site (protonated Asp or Asn with bound Na^+) is required to reconcile computations and experiment. Valences for transporters with D454A and K mutations were also calculated and are shown in Table 2.

Extracellular K^+ Binds to EAAC1 D454N but with Reduced Affinity. Based on the findings reported above, it is not possible to determine if K^+ still interacts with its binding site in EAAC1 D454N, but relocation is impaired, or if the mutation results in a transporter deficient in K^+ binding. To differentiate between these two possibilities, we tested whether extracellular Cs^+ is able to inhibit Na^+/glutamate exchange, as would be expected if Cs^+ binds to the transporter.[19] We used Cs^+ instead of K^+ because it is known to bind to the K^+ binding site, but is transported at a 2.5-fold lower rate, eliminating problems with induction of reverse transport currents that would interfere with the assay.[20,21] As shown in Figure 4A for wild-type EAAC1, anion currents were inhibited by Cs^+ with a K_i = 31 ± 7 mM in forward transport and 48 ± 2 mM in homoexchange (Figure 4A and B).

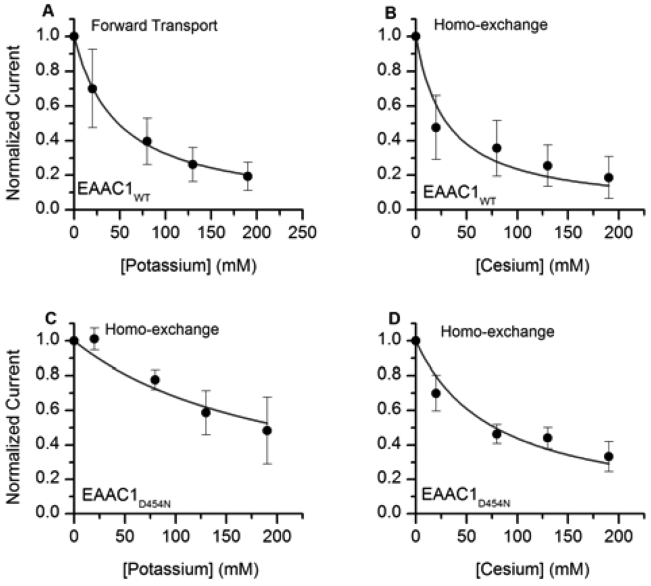

Figure 4. K^+ and Cs^+ bind to EAAC1 D454N, but with reduced affinity. Na^+/glutamate-induced anion currents were inhibited by extracellular K^+ and Cs^+ in the wild-type and mutant transporters. The extracellular solutions contained 10 mM Na^+, 1.5 mM glutamate, and varying $[K^+]$ or $[Cs^+]$ (0−190 mM). NMGMes was added to each solution to make up for the difference in ionic strength. The intracellular solutions contained 120 mM NaSCN and 10 mM glutamate. (A) Glutamate-induced EAAC1 WT anion currents in the forward transport mode were inhibited by extracellular K^+ with K_i = 31 ± 7 mM. Application of extracellular K^+ to EAAC1 WT in the homoexchange mode resulted in minimal inhibition of anion currents between 0 and 190 mM K^+, due to the simultaneous activation of reverse transport by K^+. Therefore, K^+ was substituted with Cs^+, which induces reverse transport at a slower rate, and Cs^+ inhibited anion currents with K_i = 48 ± 2 mM in the homoexchange mode (B). K^+ and Cs^+ inhibited anion currents associated with homoexchange with K_i = 210 ± 32 mM (C) and K_i = 78 ± 11 mM (D), respectively, in EAAC1 D454N. All voltages were 0 mV. The solid lines represents a fit to the function $I = K_i/([\text{cation}^+] + K_i)$.

Similar experiments were performed with EAAC1 D454N in homoexchange mode with varying extracellular $[K^+]$ and varying extracellular $[Cs^+]$. Both cations were found to be still able to interact with the K^+ binding site in EAAC1 D454N, as demonstrated by the decreased magnitude of the Na^+-induced anion currents with increasing $[K^+]$ and $[Cs^+]$ (Figure 4C and D). The anion currents were inhibited with a K_i of 210 ± 32 mM and 78 ± 12 mM, for K^+ and Cs^+, respectively. Therefore, these findings reveal that following mutation of Asp 454 to Asn, potassium and cesium can still interact with its binding site, although with somewhat reduced apparent affinity.

Effect of Mutation of Asp-454 to Ala. In contrast to findings with the EAAC1 D454N transporter, outwardly directed currents were obtained in both forward transport and exchange mode in the presence of intracellular SCN^- for EAAC1 with the less-conservative D454 to alanine mutation

(Figure 5A). These currents were caused by inhibition of the well-known leak anion conductance (inward current due to

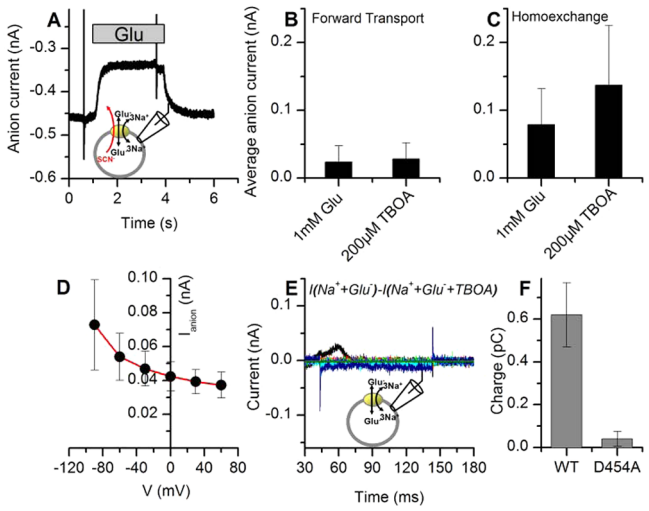

Figure 5. The less conservative D454A mutation causes a defect in glutamate translocation. (A) Glutamate application inhibits inward leak anion current in EAAC1 D454A in the presence of intracellular 120 mM NaSCN and 10 mM glutamate, causing apparent outward current. Extracellular solutions contained 140 mM Na^+. (B and C) Average inhibition of leak anion currents by glutamate or TBOA in the forward and the exchange mode. (D) $I-V$ relationship of the apparent outward current in exchange mode. (E) EAAC1-specific transient currents in response to voltage jumps (−90 to +60 mV starting from −90 mV resting potential) are absent for EAAC1 D454A in exchange mode. The pipet solution contained 120 mM NaMes and 10 mM glutamate, the extracellular solution contained 140 mM Na^+ and 1 mM glutamate. (F) Average charge obtained by integrating voltage-jump induced transient currents, such as the ones in (E) (off response).

SCN^- outflow), as indicated by the voltage dependence (Figure 5D). Average anion currents following glutamate application were of similar magnitude to those measured following application of the nontransportable inhibitor TBOA, which is known to inhibit the leak anion conductance in EAAC1 WT;[22] 24 ± 23 pA (glutamate) and 28 ± 23 pA (TBOA) for forward transport (Figure 5B), and 85 ± 54 pA (glutamate) and 137 ± 88 pA (TBOA) for homoexchange (Figure 5C). These results indicate that glutamate behaves similar to a nontransportable inhibitor in EAAC1 D454A. If glutamate cannot be transported, it is expected that charge movement associated with glutamate translocation is eliminated by the mutation. Consistent with this expectation, no transient currents associated with the rearrangement of charges in the Na^+/glutamate exchange equilibrium following a voltage jump were seen under homoexchange conditions (Figure 5E and F).

Molecular Dynamics Simulations Suggest Nonfunctional Na^+ Binding after Substitution of D454 with Ala but Not Asn. It was reported previously that a Na^+ ion is stable in the Na1 binding site of GltPh in molecular dynamics (MD) simulations up to 40 ns.[10] Our results using the EAAT3 homology model (EAAT3 is the human homologue of rat EAAC1) are consistent with these reports, showing that a Na^+ ion is stable in the corresponding Na1 site in the homology model (data not shown), independent of the occupation state of the hypothesized Na3 site. EAAT3 has 54% sequence identity and 66% sequence similarity in the c-terminal transport domain, which harbors the substrate and Na^+ binding sites. However, in the transmembrane helices, conservation is even higher with 70% identity and 80% similarity of TM7, for example. Therefore, we assume that the homology model is a reasonable starting point for MD simulations, and EAAT3-GltPh chimera models have been successfully used for MD simulations in the literature.[12]

We next performed MD simulations after altering the side chain in position 454. A Na^+ ion remained stable in the Na1 site for 20 ns when the β-carboxylate of D454 was protonated (Figure 6A, Na3 site not occupied). Similar results were

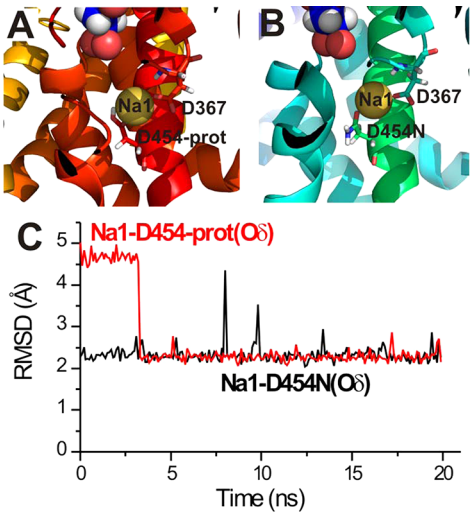

Figure 6. A sodium ion is stable in the Na1 site in the protonated state, as well as after mutation of D454 to asparagine. (A and B) Structure of the Na1 binding site in EAAC1 D454-protonated (A) and EAAC1 D454N (B) at the end of 20 ns simulations. The sodium ion is illustrated by the yellow sphere. (C) RMSD between the Na^+ ion in the Na1 site and the D454N(Oδ) atom (black) and the D454-protonated (Oδ) atom as a function of time. The Na^+ ion in the D454-protonated site was not directly located in the Na1 site after minimization, but moved into the site to remain stable there after a few nanoseconds.

obtained for the D454N exchange (Figure 6B). It is noteworthy that, in the absence of Na3 occupancy, the Na^+ binding configuration is analogous to the intermediate configuration proposed by Huang and Tajkhorshid[10] in which both D454 and D367 carboxylates contribute to cation ligation. In three out of four simulations, the Na^+ ion remained in the D454N Na1 site after the Na3 site was occupied (20 ns runs), while dissociation after ∼2 ns was observed in one run. Stability of Na^+ in the D454-protonated or D454N mutant Na1 site was independent of the occupation of the Na3 site (Supporting Information Figure 2). Furthermore, a sodium ion in the proposed Na3 site was stable in all simulations (Supporting Information Figure 2), in the absence or presence of mutations in position 454. These results suggest that sodium can still bind to the transporter with the D454N substitution, consistent with previous experimental results showing that Na^+ affinity is unchanged in the EAAC1 D454N transporter.[15]

We next tested the less conservative D454A substitution, which does not translocate glutamate at all.[13] MD simulations showed that a Na^+ ion is unstable in the Na1 site, moving away from its native position within less than 0.1 ns (Figure 7B), most likely due to the lack of coordinating O atoms. Calculating the valence, ν_{Na+}, of the D454A mutant Na1 site for Na^+ using

dx.doi.org/10.1021/cn300163p | ACS Chem. Neurosci. 2012, 3, 1073−1083

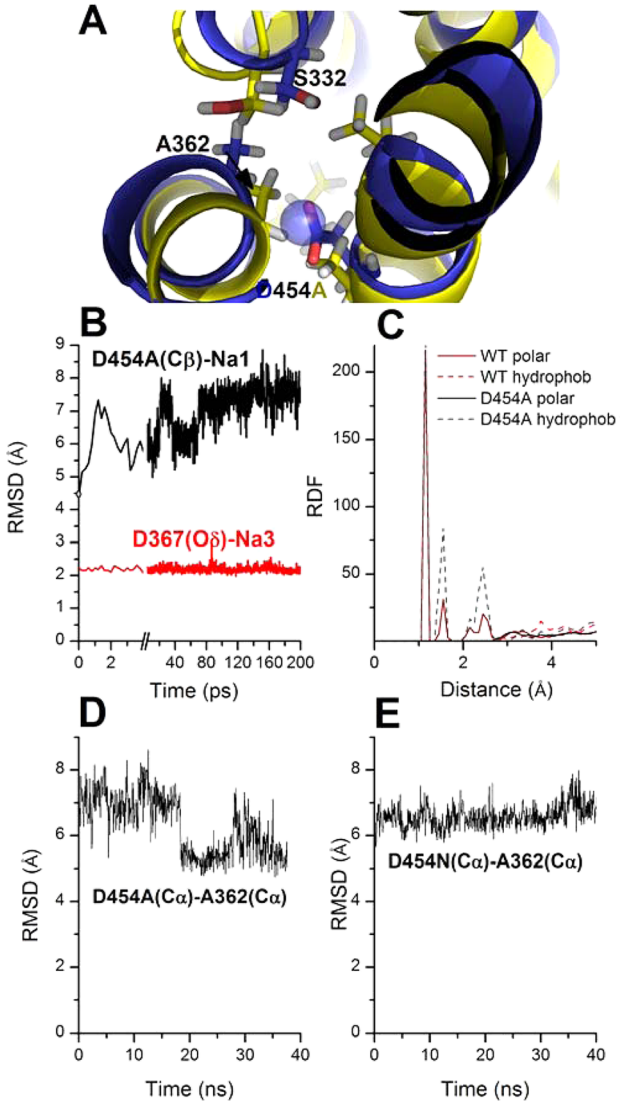

Figure 7. The substitution of D454 with alanine distorts the structure of the C-terminal transport domain by creating a hydrophobic domain in the vicinity of the D454A side chain. (A) End points of 20 ns MD simulations for EAAC1 WT (blue) and EAAC1 D454A (yellow). The Na^+ ion in the Na1 site of WT is indicated as the blue sphere (not drawn to scale). The arrow illustrates movement of the A362 residue in EAAC1 D454A toward the Na1 site. In the mutated transporter, the ion in the Na1 site has dissociated. (B) RMSD between the Na^+ ion in the Na1 site and the D454A(Cβ) atom (red), and the Na^+ ion in the Na3 site and the D367(Oδ) atom as a function of time (both in EAAC1 D454A). (C) D454(Cβ)-polar/hydrophobic radial distribution functions from MD simulations (see legend for meaning of lines). (D and E) RMSDs for D454A(Cα)-A362(Cα) (D) and D454N(Cα)-A362(Cα) (E) as a function of time.

$$\nu_{Na+} = \sum_{j=1}^{M} \nu_j = \sum_{j=1}^{M} \left(\frac{R_j}{R_0}\right)^{-N} \quad (1)$$

with N = 4.29 and R_0 = 1.622 Å for Na^+ [23] results in ν_{Na+} of 0.53 (R_j is the distance between the oxygen ligand and the cation). Restraining Na^+ in the D454A Na1 site during simulations to prevent dissociation results in some accommodation of the Na1 site, but the ν_{Na+} of 0.82 is still too small to account for significant binding.[24] In contrast to instability of the bound cation in the Na1 site, a Na^+ ion was stable in the Na3 site of EAAC1 D454A, consistent with previous results showing that Na^+ can activate the leak anion conductance in the empty mutant transporter. However, it is unclear how Na^+ would be able to access this binding site, because water is mainly excluded from the core of the transport domain by the D454A mutation (Figure 7C). Even in the *apo*-form (aspartate-free), the Na1 and Na3 sites do not become accessible to water (Figure 7C), pointing to a disruption of crucial reaction steps necessary for transport by the D454A mutation, which is much more severe than in the case of the D454N mutation. Interestingly, the simulations also point to instability of a Na^+ ion in the EAAC1 D454A Na2 site. These results may explain the dramatic, about 10-fold reduction of apparent affinity of this mutant transporter for glutamate, because substrate binding and Na^+ binding to the Na2 site are, most likely, cooperative.

In order to better understand the effect of the D454A mutation on transport, we inspected trajectories of amino acid residues in the vicinity of the D454A side chain from 40 ns MD simulations. While the positions of the hydrophobic side chains V358 and V451 with respect to D454 are not significantly altered by the alanine substitution, A362 moves significantly closer to D454 compared to the wild-type, as well as the D454N mutant transporter (Figure 7D and E), most likely to at least partially compensate for the void left by the missing carboxylate and the dissociated Na^+ ion. This compensation is caused by a bending and partial rotation of the top of the α-helical part of TM7a toward TM8 (Figure 7A). In addition, the side-chain OH group of the serine residue 332 on the tip of RL1 rotates in EAAC1 D454A to point away from the interior of the protein (Figure 7A). Together, these subtle, but significant structural changes create a fully hydrophobic environment of the D454A residue, prohibiting the existence of an aqueous access pathway to the binding site, which would, most likely, be required for Na^+ association.

A Transporter with the D454K Mutation Is Still Partially Functional. The previous results suggest that the protonated D454 side chain contributes as a ligand to the Na1 site, rendering the overall charge of the ligand−Na^+ complex +1. If this is the case, it is possible that a basic, positively charged lysine side chain in position 454 can substitute for the Na^+ ion, as seen previously in a proton-dependent homologue of the sodium-dependent transporter LeuT.[25] Consistent with this hypothesis, MD simulations of EAAC1 with the D454K substitution show that the positively charged $-NH_3^+$ group takes the place of the Na^+ cation (Figure 8A). As expected, Na^+ in the Na1 site is not stable in this mutant transporter. As in the wild-type transporter with Na1 occupied, water is excluded from the vicinity of the lysine $-NH_3^+$ group, as illustrated by the radial distribution function (Figure 8B). In contrast, water can readily penetrate the Na1 site of the *apo*-form (absence of Na^+) of EAAC1 D454N (Figure 8B, blue line), consistent with previous simulation results obtained for the *apo*-form of GltPh.

While forward transport in the EAAC1 D454K mutant transporter was not functional (I(transport) = −1 ± 2 pA), glutamate was clearly able to interact with the transporter, although with dramatically reduced apparent affinity (K_m = 1.1 ± 0.6 mM) compared to the wild-type transporter (K_m = 8 μM). TBOA was also able to bind to the mutant transporter with a 10-fold reduced K_m of 6 ± 2 μM (data not shown). As found for the transporter with the D454A mutation, glutamate application to EAAC1 D454K resulted in inhibition of the leak anion current at steady-state (Figure 8D). However, a transient inward anion current was observed upon rapidly jumping the

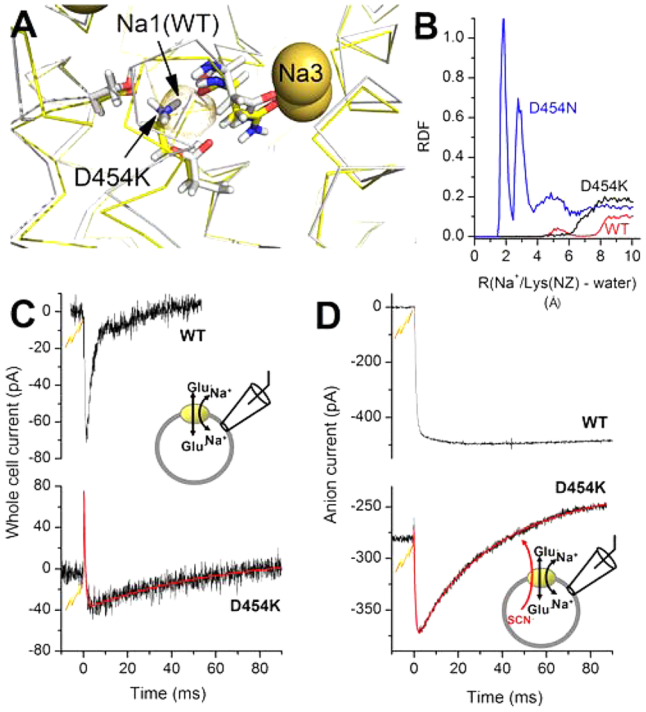

Figure 8. A lysine side chain amine function in position D454 can replace Na^+ bound to the Na1 site. (A) End point of a 20 ns MD simulation after substitution of D454 with lysine. The EAAC1 WT structure superposition demonstrates that the lysine side chain NH_3^+ occupies the Na1 site (Na^+ ion bound in the WT shown in dot representation). The Na^+ ions in the Na3 sites are shown as yellow spheres. (B) D454K(NZ)(black)/Na^+(red)−water(O) radial distribution functions from MD simulations. For comparison, the D454N-(Oδ)−water RDF is shown for the *apo*-form (blue), demonstrating water permeation into the Na1 site, as proposed previously. (C) Transient currents observed upon laser photolysis of MNI-caged glutamate at time t = 0 ms in EAAC1 WT (top) and EAAC1 D454K (bottom). The cell contained 120 mM NaMes/10 mM glutamate. The extracellular solution contained 140 mM NaMes (V = 0 mV). (D) Anion current response to a [glutamate] jump at t = 0 ms for EAAC1 WT (top) and EAAC1 D454K (bottom). Conditions as in (C), but the intracellular solution contained 120 mM NaSCN/10 mM glutamate.

glutamate concentration (Figure 8D), indicating that glutamate can still activate the anion conductance.

In exchange mode, in the absence of a permeating anion, a slowly decaying inward transient current was observed after glutamate application (Figure 8C). This current decayed with a time constant of 65 ± 10 ms, which is about 10-fold slower decay than that of wild-type EAAC1. This result suggests that the initial partial reactions associated with amino acid exchange are still functional in EAAC1 D454K.

DISCUSSION

The role of the highly conserved amino acid residue, D454, which forms a ligand of the bound Na^+ ion, participating in the proposed Na1 site, has been controversially discussed in the literature.[13,15,26] On one hand, mutation of the homologous residue D405 in GltPh to asparagine was shown to abolish Tl^+ binding to the Na1 site.[7] Furthermore, the Na^+/glutamate coupling ratio was reduced, pointing to a contribution of this side chain not only to Tl^+ binding, but also to Na^+ binding.[7] On the other hand, it was found that the D454N mutation in EAAC1 had little effect on the affinity of the *apo*-form of the transporter for Na^+,[15] and the asparagine substitution as well as other conservative mutations were still functional in Na^+-dependent substrate exchange, as measured by radiolabeled substrate flux in proteoliposomes.[13] Our results presented here clarify some of these issues, showing directly that the D454N mutation is electrically fully functional in the Na^+/glutamate homoexchange mode (Figure 1) with similar charge being moved in the translocation step(s) compared to the wild-type transporter (Figure 2). These results indicate that the D454N mutant transporter is in terms of the translocation process electrostatically equivalent to the wild-type transporter, which can be explained by assuming that the D454 side chain is protonated under physiological conditions. If this is the case, then the net charge of the nonoccupied Na1 site is 0.

Consistent with the hypothesis of a noncharged, neutral nature of the Na1 site, calculations of the pK_a of the D454 side chain using empirical as well as continuum electrostatics-based methods yielded values >8.3 in the Na^+-bound form (Table 1). In the *apo*-state, predicted pK_a values were slightly lower, but still favorable for protonation at pH 7.3. Interestingly, D454 was the only highly conserved ionizable amino acid side chain within the transmembrane domain, for which deviation from the protonation state predicted from an aqueous environment was found. Only D312 (analogous to D367 in EAAC1) was predicted to have somewhat higher pK_a values than those in water, most likely due to its location buried deeply within the membrane. This side chain was previously proposed to contribute to the potential third Na^+ binding site, the Na3 site.[11] Consistent with D454 protonation, we found that the pH dependence of EAAC1 D454N was unchanged compared to the wild-type transporter, suggesting that the protonation state does not change within a pH range of 5−9. This result is in agreement with this side chain only becoming deprotonated at pH values larger than 9, according to a highly perturbed pK_a.

In contrast to the lack of Tl^+ binding found for GltPh with the D405N mutation, our results suggest that Na^+ still binds to the mutated Na1 site. This conclusion is based on the evidence for functional translocation step(s) (Figures 1E and 2), as well as the MD simulations showing that a Na^+ ion is stable in the Na1 site in the D454N mutant transporter, as well as in the D454-protonated state (Figure 6). Previous results by the Kanner laboratory[13] also point to functional binding of Na^+ to transporters with conservative D454 mutations, because exchange was observed in the sole presence of Na^+, but not Li^+. This result indicated that the selectivity of the Na1 site for Na^+/Li^+ was altered by the mutations, without abolishing Na^+ binding. Together, these results indicate that mutations to amino acids that can provide a side chain oxygen ligand to Na^+ coordination may still have intact Na^+ binding at the Na1 site, because the overall electrostatics of the binding site are unchanged by these mutations. In contrast, the more severe D454A exchange results in dramatic impairment of the transport process, with a transporter that is unable to translocate glutamate (Figure 5A). Consistently, MD simulations illustrate a distortion of the Na1 site in EAAC1 D454A (Figure 7A), which is caused by immediate dissociation of the Na^+ ion placed in the Na1 site, followed by a hydrophobic collapse of the site, excluding water and potential ligands for coordination of cations. Therefore, it is likely that EAAC1 D454A is unable to coordinate cations in the Na1 site, resulting in the defect of glutamate translocation, for which an occupied Na1 site is most likely required. Simulations indicate that Na^+

can still bind to the Na3 site in the D454A mutant transporter. However, due to the hydrophobic collapse of the D454A Na1 site, it is unclear how a Na^+ ion could access this site. It is possible that the D454A mutation causes structural effects on time scales that are beyond the capability of the present simulations.

Relocation of the empty transporter to the outward facing conformation is driven by the K^+ concentration gradient, and K^+ binding initiates the relocation reaction.[27] The overall rate for this process depends on two factors: the saturation of the K^+ binding site and the intrinsic rate constant associated with the relocation process. It was previously proposed that the D454 side chain contributes to a cation binding site that can bind both Na^+ and K^+.[13] Our data showing a moderate decrease in the apparent affinity for K^+ and Cs^+ caused by the D454N mutations are consistent with this proposal (Figure 4C and D). However, our results indicate that the reduction of the rate of K^+-induced relocation is caused by two mechanisms: (1) Moderate reduction of the affinity for K^+, resulting in lower % saturation of the K^+-binding site at physiological internal $[K^+]$ and (2) reduction of the intrinsic rate constant of the relocation step(s). Such a reduction of the relocation rate constant is not surprising, considering that the translocation step is also slowed about 3-fold by the mutation. Given the relatively low K_m of EAAC1 for internal K^+,[20] the mutation would result in a reduction of percent of saturation of the K^+ binding site from 50% to 33%, which cannot account for the full effect on the relocation rate. However, taking also into account the reduction of the intrinsic relocation rate constant by the mutation, an apparent relocation rate that is about 4.5−5-fold slower than that in the wild-type transporter is estimated, a value that accounts reasonably well for the experimental data. This value is also consistent with previous data showing that net flux is not completely abolished in EAAC1 D454N,[13] indicating that relocation is associated with a nonzero rate.

The hypothesis proposed here is that the side chain of D454 can be protonated in the Na^+-bound state of the Na1 site. This requires a pK_a shift of several orders of magnitude, resulting in a stabilization of the protonated carboxylate by about 20−50 kJ/mol compared to the aqueous environment. Such large pK_a shifts of carboxylate side chains are not uncommon in enzymes, as well as membrane proteins, with prominent examples being catalytically active Asp side chains in bacteriorhodopsin[28,29] and the carboxylates contributing to Na^+/K^+ coordination on the Na^+/K^+ ATPase.[30] The protonation state of these carboxylates was proposed to contribute to cation selectivity of these sites. Modulation of the protonation state may also be important for the Na1 site of glutamate transporters, although it is unlikely that the site is involved in proton co-transport, as indicated by the unchanged pH dependence of glutamate binding by EAAC1 D454N. If changes in protonation state of D454 occur, then they are likely to involve protonation/H^+ dissociation from the same side of the membrane, rather than directional proton transfer.

Interestingly, a transporter with the D454K substitution was still somewhat functional (Figure 8). Although no steady-state transport was observed, some pre-steady-state charge movement as well as anion conductance was observed in the homoexchange mode. Together with MD simulations suggesting that the protonated side chain amino group can replace Na^+ in the Na1 site, these results further support the hypothesis that the overall charge of the occupied Na1 site, either with Na^+ or with the $-NH_3^+$ group from lysine, is +1. Lack of steady-state transport is evident in this interpretation, because the $-NH_3^+$ group would behave as a permanently bound cation in the Na1 site. Thus, no dissociation of cation and binding of K^+ can take place, eliminating the relocation process.

CONCLUSIONS

In summary, we have demonstrated the subtle effects of conservative mutations, such as the Asp to Asn exchange, to the D454 residue. The mutation is predicted to result in charge conservation of the Na1 site because the D454 side chain is protonated under physiological conditions, with a computed pK_a value of >8. Consistently, MD simulations predict that a lysine amino function in position D454 can substitute for the bound cation, producing a transporter that can still catalyze charge movement in the Na^+/glutamate homoexchange mode. Our results are consistent with a model of an overlapping Na^+/K^+ site deeply buried in the transporter, to which D454 contributes a side chain oxygen atom. Due to the protonated, neutral D454 side chain, the net charge of the occupied Na1 site is predicted to be +1.

METHODS

Molecular Biology. Rat EAAC1 wild type and mutant constructs were subcloned into the pBK-CMV vector (Strategene) as described previously.[31] The wild type and mutant constructs were transiently transfected into subconfluent HEK293 (ATCC Number: CRL 1573) cells, using Fugene 6 transfection reagent according to the supplier's protocol. Electrophysiological studies were performed 1−2 days after transfection.

Electrophysiology. Whole cell current recordings for the EAAC1 induced anion currents were carried out under voltage clamp conditions. All experiments were performed under homoexchange for EAAC1 D454N, due to inability of the mutant transporter to catalyze steady-state transport currents. The recording pipet resistances were 2−3 MΩ.

pH Dependent Ionic Conditions. The pH of the extracellular solutions was varied from pH 6.0 to pH 9.0 and contained 140 mM NaCl, 2 mM $MgCl_2$, 2 mM $CaCl_2$, 15 mM tris(hydroxymethyl)-aminomethane (TRIS), and 15 mM 2-(*N*-morpholino)ethanesulfonic acid (MES). NaOH or HCl was used to adjust the solutions to the desired pH. For each pH, glutamate concentration jumps were applied at 0 mV. The pipet solution contained 140 mM NaSCN, 2 mM $MgMes_2$ (Mes = methanesulfonate), 5 mM ethylene glycol-bis(2-aminoethylether)-*N*,*N*,*N*′,*N*′-tetraacetic acid (EGTA), 10 mM 4-(2-hydroxyethyl)piperazine-1-ethanesulfonic acid (HEPES), and 10 mM glutamate.

Ionic Conditions for Extracellular K^+ inhibition. Na^+/glutamate exchange was achieved by applying saturating Na^+ and glutamate concentrations on both sides of the membrane. This locks the transporter in the Na^+/glutamate translocation branch and the K^+ bound states are no longer accessible. The intracellular solution contained 120 mM NaSCN, 2 mM $MgMeS_2$, 5 mM EGTA, 10 mM HEPES, and 10 mM glutamate. The extracellular solution contained 10 mM NaMes, 1.5 mM glutamate, and varying $[K^+]/[Cs^+]$ (0−190 mM). NMGMes (NMG = *N*-methyl-D-glucamine) was added to each solution to make up for the difference in ionic strength.

The effect of varying the extracellular $[K^+]$ on anion currents in the forward transport mode was tested for EAAC1 WT. The pipet solution contained 115 mM KSCN. The extracellular solution was identical to that under homoexchange conditions.

Voltage Jumps. Voltage jumps (−90−60 mV) were applied to perturb the Na^+/glutamate exchange equilibrium. Transient currents resulting from relaxation to a new equilibrium were recorded, and unspecific currents in the presence of nontransportable competitive inhibitor TBOA (DL-*threo*-*β*-benzyloxyaspartic acid) subtracted to obtain the EAAC1 specific component. The pipet solution contained 120 mM NaMes, 2 mM $MgMes_2$, 5 mM EGTA, 10 mM HEPES, and

10 mM glutamate. The extracellular solution contained 140 mM NaMes, 1 mM glutamate, and 200 μM TBOA.

Nonspecific transient currents were subtracted in Clampfit and the EAAC1 specific component fit to a Boltzmann-like function:

$$Q(V_m) = Q_{min} + Q_{max}[1 + \exp(Z_Q(V_Q - V_m)F/(RT))]^{-1} \quad (2)$$

Here, Q represents the charge moved, Z_Q the valence of this charge, and V_Q the midpoint potential of the charge movement. R is the gas constant, T the temperature, and F the Faraday constant.

Laser Pulse Photolysis and Rapid Solution Exchange. Laser pulse photolysis experiments were performed as previously described.[32] 4-Methoxy-7-nitroindolinyl (MNI)-caged glutamate (TOCRIS) was applied to the cells using a small quartz tube and then photolyzed with a light flash (355 nm Nd:YAG laser, Minilite series; Continuum, Santa Clara, CA) delivered through an optical fiber (350 μm diameter). The MNI-caged glutamate solutions were freshly prepared before starting each experiment. The yield from the photolysis of 1 mM MNI-caged glutamate was calibrated to release 200 μM free glutamate for the maximum laser energy, according to the previously described procedure.[31] Neutral density filters were applied to adjust the laser energy and attenuate glutamate release.

pK_a Calculations. We used multiconformational continuum electrostatics (MCCE, ref 17) and the PROPKA 3.1 server (http://propka.ki.ku.dk/, ref 16) to estimate pK_a values of buried, ionizable side chains of GltPh. For a detailed description of MCCE see ref 17. Briefly, MCCE uses continuum electrostatics (Delphi, ref 33) to calculate electrostatic solvation energies of buried side chains while varying the conformation of the side chains at different pH values. For our calculations, we have used protein dielectric constants of 4 and 8.

Molecular Dynamics. The model system for MD simulations was set up using VMD[34] by placing a EAAT3 homology model based on the GltPh structure (PDB code 2NWX,[7] 2 Na^+ ions, and 1 aspartate bound to each subunit) into a pre-equilibrated POPC lipid bilayer with the dimensions 130 × 130 Å^2. Sequence alignment was performed with ClustalW,[35] and the homology model was built with Modeler.[36] TIP3P water was added to generate a box measuring 100 Å in the z direction. Finally, NaCl was added at a concentration of 150 mM. The total system contained 146 859 atoms. The system was first equilibrated in a NVT simulation (volume and temperature constant) using NAMD 2.8b[37] with everything except the lipid tails fixed (1 ns). Subsequently, the system was equilibrated for 4 ns at constant pressure of 1 atm and constant temperature (NPT), using Langevin dynamics. For the following production runs, we used NPT conditions (1 atm), but holding the lipid bilayer area constant. The cutoff for short-range interactions was 12 Å. For electrostatic interactions, we used the particle mesh Ewald method[38] implemented in NAMD. Bonds including hydrogen atoms and TIP3P water were kept rigid using SHAKE. The time step of the simulations were 2 fs. All simulations were performed using the CHARMM27 force field.[39]

Computation of the Valence of the Transport Domain. We have used the adaptive Poisson−Boltzmann solver, APBS,[40] together with the APBSmem Java routines[41] for the calculation of electrostatic energies of the glutamate transporter embedded into an implicit membrane. In the presence of an internal membrane potential, V, the following modified version of the linearized Poisson−Boltzmann equation (LPBE) is used, according to the formalism first introduced by Roux:[42]

$$-\nabla[\varepsilon(\vec{r})\nabla\phi(\vec{r})] + \bar{\kappa}^2(\vec{r})\,\phi(\vec{r}) = \frac{e4\pi}{k_B T}\left(\rho(\vec{r}) + \frac{\bar{\kappa}^2 V}{4\pi} f(\vec{r})\right) \quad (3)$$

Here, ε is the dielectric constant, which depends on the spatial coordinate, $\phi = e\Phi/k_BT$, where Φ is the electrostatic potential, e the elementary charge, T the temperature, and k_B the Boltzmann constant. κ is the Debye−Hückel screening constant, and ρ is the charge density. f(r) is the Heaviside step function, set to 1 in the intracellular solution and is 0 in the membrane, protein, and extracellular solution. Details of the method can be found in ref 41.

The total electrostatic energy, E, is then computed by summing up over the product of the local charge and the potential:[43]

$$E = \int \phi(\vec{r})\,\rho(\vec{r})\,dV \quad (4)$$

where dV is the volume element. To compute the valence, membrane potentials of varying magnitude, V, are applied to the internal side of the membrane, and the difference in total electrostatic energy, ΔE, for two protein configurations, for example, inward- and outward-facing conformations, is calculated. When plotting ΔE versus the membrane potential, the valence is obtained from the slope.[44] Energy contributions that do not come from movement of protein charges have been subtracted in this approach, after calculating the electrostatic energy in the absence of protein charges. The details of the APBSmem setup are described in the Supporting Information.

The APBSmem approach was validated by using a model system, in which a Na^+ ion was moved from the water phase into a membrane of 30 Å thickness at a distance of 10 Å below the membrane surface. As expected, the valence of this transition was 0.32.

■ ASSOCIATED CONTENT

Supporting Information

Additional figures and details as described in the text. This material is available free of charge via the Internet at http://pubs.acs.org.

■ AUTHOR INFORMATION

Corresponding Author

*Mailing address: Department of Chemistry, Binghamton University, 4400 Vestal Parkway East, Binghamton, NY 13902. Phone: (607) 777-3250. Fax: (607) 777-4478. E-mail: cgrewer@binghamton.edu.

Present Address

†1001 Rockville Pike #105, Rockville, MD 20852.

Funding

This work was supported by the National Institutes of Health Grant 2R01NS049335-06A1 awarded to C.G. and a Binational Science Foundation (BSF) Grant 2007051 awarded to C.G. and Baruch I. Kanner.

Notes

The authors declare no competing financial interest.

■ ACKNOWLEDGMENTS

We are grateful to C. Zander for assistance with the PB calculations.

■ ABBREVIATIONS

EAAC1, excitatory amino acid carrier 1; EAAT3, excitatory amino acid transporter 3; GltPh, glutamate transporter homologue from *Pyrococcus horikoshii*; TBOA, DL-*threo*-β-benzyloxyaspartic acid; MD, molecular dynamics; APBS, adaptive Poisson−Boltzmann solver; PB, Poisson−Boltzmann

■ REFERENCES

(1) Kanner, B. I., and Sharon, I. (1978) Active transport of L-glutamate by membrane vesicles isolated from rat brain. *Biochemistry 17* (19), 3949−3953.

(2) Zerangue, N., and Kavanaugh, M. P. (1996) Flux coupling in a neuronal glutamate transporter. *Nature 383* (6601), 634−637.

(3) Kanner, B. I., and Zomot, E. (2008) Sodium-coupled neurotransmitter transporters. *Chem. Rev. 108* (5), 1654−1668.

(4) Levy, L. M., Warr, O., and Attwell, D. (1998) Stoichiometry of the glial glutamate transporter GLT-1 expressed inducibly in a Chinese hamster ovary cell line selected for low endogenous Na+-dependent glutamate uptake. *J. Neurosci. 18* (23), 9620−9628.

(5) Kanner, B. I., and Bendahan, A. (1982) Binding order of substrates to the sodium and potassium ion coupled L-glutamic acid transporter from rat brain. *Biochemistry 21* (24), 6327−6330.
(6) Yernool, D., Boudker, O., Jin, Y., and Gouaux, E. (2004) Structure of a glutamate transporter homologue from Pyrococcus horikoshii. *Nature 431* (7010), 811−818.
(7) Boudker, O., Ryan, R. M., Yernool, D., Shimamoto, K., and Gouaux, E. (2007) Coupling substrate and ion binding to extracellular gate of a sodium-dependent aspartate transporter. *Nature 445* (7126), 387−393.
(8) Bastug, T., Heinzelmann, G., Kuyucak, S., Salim, M., Vandenberg, R. J., and Ryan, R. M. (2012) Position of the third Na+ site in the aspartate transporter GltPh and the human glutamate transporter, EAAT1. *PLoS One 7* (3), e33058.
(9) Groeneveld, M., and Slotboom, D. J. (2010) Na(+):aspartate coupling stoichiometry in the glutamate transporter homologue Glt(Ph). *Biochemistry 49* (17), 3511−3513.
(10) Huang, Z., and Tajkhorshid, E. (2010) Identification of the third Na+ site and the sequence of extracellular binding events in the glutamate transporter. *Biophys. J. 99* (5), 1416−1425.
(11) Tao, Z., Rosental, N., Kanner, B. I., Gameiro, A., Mwaura, J., and Grewer, C. (2010) Mechanism of cation binding to the glutamate transporter EAAC1 probed with mutation of the conserved amino acid residue Thr101. *J. Biol. Chem. 285* (23), 17725−17733.
(12) Larsson, H. P., Wang, X., Lev, B., Baconguis, I., Caplan, D. A., Vyleta, N. P., Koch, H. P., Diez-Sampedro, A., and Noskov, S. Y. (2010) Evidence for a third sodium-binding site in glutamate transporters suggests an ion/substrate coupling model. *Proc. Natl. Acad. Sci. U.S.A. 107* (31), 13912−13917.
(13) Teichman, S., Qu, S., and Kanner, B. I. (2009) The equivalent of a thallium binding residue from an archeal homolog controls cation interactions in brain glutamate transporters. *Proc. Natl. Acad. Sci. U.S.A. 106* (34), 14297−14302.
(14) Watzke, N., Bamberg, E., and Grewer, C. (2001) Early intermediates in the transport cycle of the neuronal excitatory amino acid carrier EAAC1. *J. Gen. Physiol. 117* (6), 547−562.
(15) Tao, Z., Zhang, Z., and Grewer, C. (2006) Neutralization of the aspartic acid residue Asp-367, but not Asp-454, inhibits binding of Na+ to the glutamate-free form and cycling of the glutamate transporter EAAC1. *J. Biol. Chem. 281* (15), 10263−10272.
(16) Li, H., Robertson, A. D., and Jensen, J. H. (2005) Very fast empirical prediction and rationalization of protein pKa values. *Proteins 61* (4), 704−721.
(17) Georgescu, R. E., Alexov, E. G., and Gunner, M. R. (2002) Combining conformational flexibility and continuum electrostatics for calculating pK(a)s in proteins. *Biophys. J. 83* (4), 1731−1748.
(18) Watzke, N., Rauen, T., Bamberg, E., and Grewer, C. (2000) On the mechanism of proton transport by the neuronal excitatory amino acid carrier 1. *J. Gen. Physiol. 116* (5), 609−622.
(19) Grewer, C., Watzke, N., Rauen, T., and Bicho, A. (2003) Is the glutamate residue Glu-373 the proton acceptor of the excitatory amino acid carrier 1? *J. Biol. Chem. 278* (4), 2585−2592.
(20) Grewer, C., Zhang, Z., Mwaura, J., Albers, T., Schwartz, A., and Gameiro, A. (2012) Charge compensation mechanism of a Na +-coupled, secondary-active glutamate transporter. *J. Biol. Chem. XX*, xxx−xxx.
(21) Bergles, D. E., Tzingounis, A. V., and Jahr, C. E. (2002) Comparison of coupled and uncoupled currents during glutamate uptake by GLT-1 transporters. *J. Neurosci. 22* (23), 10153−10162.
(22) Shimamoto, K., Lebrun, B., Yasuda-Kamatani, Y., Sakaitani, M., Shigeri, Y., Yumoto, N., and Nakajima, T. (1998) DL-*threo*-*β*-benzyloxyaspartate, a potent blocker of excitatory amino acid transporters. *Mol. Pharamcol. 53* (2), 195−201.
(23) Page, M. J., and Di Cera, E. (2006) Role of Na+ and K+ in enzyme function. *Physiol. Rev. 86* (4), 1049−1092.
(24) Nayal, M., and Di Cera, E. (1996) Valence screening of water in protein crystals reveals potential Na+ binding sites. *J. Mol. Biol. 256* (2), 228−234.
(25) Shaffer, P. L., Goehring, A., Shankaranarayanan, A., and Gouaux, E. (2009) Structure and mechanism of a Na+-independent amino acid transporter. *Science 325* (5943), 1010−1014.
(26) Tao, Z., Gameiro, A., and Grewer, C. (2008) Thallium ions can replace both sodium and potassium ions in the glutamate transporter excitatory amino acid carrier 1. *Biochemistry 47* (48), 12923−12930.
(27) Kavanaugh, M. P., Bendahan, A., Zerangue, N., Zhang, Y., and Kanner, B. I. (1997) Mutation of an amino acid residue influencing potassium coupling in the glutamate transporter GLT-1 induces obligate exchange. *J. Biol. Chem. 272* (3), 1703−1708.
(28) Richter, H. T., Brown, L. S., Needleman, R., and Lanyi, J. K. (1996) A linkage of the pKa's of asp-85 and glu-204 forms part of the reprotonation switch of bacteriorhodopsin. *Biochemistry 35* (13), 4054−4062.
(29) Szaraz, S., Oesterhelt, D., and Ormos, P. (1994) pH-induced structural changes in bacteriorhodopsin studied by Fourier transform infrared spectroscopy. *Biophys. J. 67* (4), 1706−1712.
(30) Yu, H., Ratheal, I. M., Artigas, P., and Roux, B. (2011) Protonation of key acidic residues is critical for the K(+)-selectivity of the Na/K pump. *Nat. Struct. Mol. Biol. 18* (10), 1159−1163.
(31) Grewer, C., Watzke, N., Wiessner, M., and Rauen, T. (2000) Glutamate translocation of the neuronal glutamate transporter EAAC1 occurs within milliseconds. *Proc. Natl. Acad. Sci. U.S.A. 97* (17), 9706−9711.
(32) Grewer, C., Gameiro, A., Zhang, Z., Tao, Z., Braams, S., and Rauen, T. (2008) Glutamate forward and reverse transport: from molecular mechanism to transporter-mediated release after ischemia. *IUBMB Life 60* (9), 609−619.
(33) Gilson, M. K., and Honig, B. (1988) Calculation of the total electrostatic energy of a macromolecular system: solvation energies, binding energies, and conformational analysis. *Proteins 4* (1), 7−18.
(34) Humphrey, W., Dalke, A., and Schulten, K. (1996) VMD: visual molecular dynamics. *J. Mol. Graphics 14* (1), 33−38, () 27−28.
(35) Thompson, J. D., Higgins, D. G., and Gibson, T. J. (1994) CLUSTAL W: improving the sensitivity of progressive multiple sequence alignment through sequence weighting, position-specific gap penalties and weight matrix choice. *Nucleic Acids Res. 22* (22), 4673−4680.
(36) Sali, A., and Blundell, T. L. (1993) Comparative protein modelling by satisfaction of spatial restraints. *J. Mol. Biol. 234* (3), 779−815.
(37) Phillips, J. C., Braun, R., Wang, W., Gumbart, J., Tajkhorshid, E., Villa, E., Chipot, C., Skeel, R. D., Kale, L., and Schulten, K. (2005) Scalable molecular dynamics with NAMD. *J. Comput. Chem. 26* (16), 1781−1802.
(38) Darden, T., York, D. M., and Pdersen, L. (1993) Particle mesh Ewald: An N log(N) method for Ewald sums in large systems. *J. Chem. Phys. 98*, 10089−10092.
(39) MacKerell, A. D., Bashford, D., Bellott, Dunbrack, R. L., Evanseck, J. D., Field, M. J., Fischer, S., Gao, J., Guo, H., Ha, S., Joseph-McCarthy, D., Kuchnir, L., Kuczera, K., Lau, F. T. K., Mattos, C., Michnick, S., Ngo, T., Nguyen, D. T., Prodhom, B., Reiher, W. E., Roux, B., Schlenkrich, M., Smith, J. C., Stote, R., Straub, J., Watanabe, M., Wiórkiewicz-Kuczera, J., Yin, D., and Karplus, M. (1998) All-Atom Empirical Potential for Molecular Modeling and Dynamics Studies of Proteins†. *J. Phys. Chem. B 102* (18), 3586−3616.
(40) Baker, N. A., Sept, D., Joseph, S., Holst, M. J., and McCammon, J. A. (2001) Electrostatics of nanosystems: application to microtubules and the ribosome. *Proc. Natl. Acad. Sci. U.S.A. 98* (18), 10037−10041.
(41) Callenberg, K. M., Choudhary, O. P., de Forest, G. L., Gohara, D. W., Baker, N. A., and Grabe, M. (2010) APBSmem: a graphical interface for electrostatic calculations at the membrane. *PLoS One 5* (9), e12722.
(42) Roux, B. (1997) Influence of the membrane potential on the free energy of an intrinsic protein. *Biophys. J. 73* (6), 2980−2989.
(43) Silva, J. R., Pan, H., Wu, D., Nekouzadeh, A., Decker, K. F., Cui, J., Baker, N. A., Sept, D., and Rudy, Y. (2009) A multiscale model linking ion-channel molecular dynamics and electrostatics to the

cardiac action potential. *Proc. Natl. Acad. Sci. U.S.A. 106* (27), 11102−11106.
(44) Choudhary, O. P., Ujwal, R., Kowallis, W., Coalson, R., Abramson, J., and Grabe, M. (2010) The electrostatics of VDAC: implications for selectivity and gating. *J. Mol. Biol. 396* (3), 580−592.